Capillarity

Vol. 8, No. 1, p. 11-22, 2023

Original article

Stress sensitivity of multiscale pore structure of shale gas reservoir under fracturing fluid imbibition

Mingjun Chen[1]*, Maoling Yan[1], Yili Kang[1], Wangkun Cao[2], Jiajia Bai[3], Peisong Li[1]

[1]*State Key Laboratory of Oil and Gas Reservoir Geology and Exploitation, Southwest Petroleum University, Chengdu 610500, P. R. China*
[2]*Institute of Engineering Technology, Petro China Coalbed Methane Company Limited, Xi'an 710082, P. R. China*
[3]*Petroleum Engineering School, Changzhou University, Changzhou 213164, P. R. China*

Keywords:
Shale gas
fracturing fluid
imbibition
stress sensitivity
pore structure

Cited as:
Chen, M., Yan, M., Kang, Y., Cao, W., Bai, J., Li, P. Stress sensitivity of multiscale pore structure of shale gas reservoir under fracturing fluid imbibition. Capillarity, 2023, 8(1): 11-22.
https://doi.org/10.46690/capi.2023.07.02

Abstract:
Generally, huge amounts of fracturing fluid are used in a shale gas well but the flowback efficiency is low. Since the distribution characteristics of imbibed fracturing fluid in shale are complex, they need further evaluation. This paper takes the Longmaxi Shale as the research object, including matrix cores, natural fracture cores and cores of artificial fracture with proppant. Stress sensitivity experiments are carried out on the above three kinds of cores under different degrees of imbibition and retention state of fracturing fluid. The results show that when the degree of aqueous phase retention is 0-0.78 pore volume, water mainly appears in the pores with a diameter of 2-50 nm. As the water saturation increases to more than 0.9 pore volume, the amounts of aqueous phase in the pores or fractures with a hydraulic diameter of 100-1,000 nm and larger than 1,000 nm increase significantly. Both the stress sensitivity of nanopores and natural fractures are enhanced by aqueous phase retention. With the increase in effective stress, the permeability damage rate of artificial fracture cores with proppant is inversely proportional to the degree of fracturing fluid retention. Aqueous phase retention in the pores with a diameter of 2-50 nm significantly contributes to the stress sensitivity of matrix cores. With the increase in effective stress, aqueous phase retention in pores with diameter larger than 100 nm increases the stress sensitivity of natural fracture cores. It is recommended that the retention degree of fracturing fluid in a shale gas reservoir should be controlled below 0.5 pore volume. In this case, the stress sensitivity of natural fractures will be less aggravated by fracturing fluid retention, and the stress sensitivity of artificial fracture with proppant will be reduced to a certain extent.

1. Introduction

Shale gas has become a vital alternative resource for extended natural gas storage (Zhou et al., 2018a; Zou et al., 2020). With regards to the economic development of shale gas, staged hydraulic fracturing has a significant time requirement, resulting in a large fracture network. Extensive fracturing fluid imbibition and low flowback efficiency can result in large amounts of aqueous phase remaining in the reservoir (Edwards and Celia, 2018; Zeng et al., 2020; Lin et al., 2021; Zhang et al., 2021). Fracturing fluid retention could reduce the gas flow capacity in shales with complex pore structure (Shaoul et al., 2011; Gasparik et al., 2012; Liu et al., 2020; Sheng et al., 2020). In the absence of external energy, shale gas wells are produced under their own pressure (Shi et al., 2022; Xu et al., 2022). This will lead to reduced formation pressure and reservoir stress sensitivity, restricting the long-term and efficient exploitation of shale gas (Zhang et al., 2018; Han et al., 2021; Rashid et al., 2022). Therefore, investigating the shale stress sensitivity mechanism under the condition of fracturing fluid retention is of great significance. In addition, it is helpful for the formulation of a reasonable production

Yandy Scientific Press

*Corresponding author.
E-mail address: chenmj1026@163.com (M. Chen); maolingyanswpu@foxmail.com (M. Yan); cwctkyl@163.com (Y. Kang); caowangkun@petrochina.com.cn (W. Cao); baijiajiaa@163.com (J. Bai); lipeisong98315@foxmail.com (P. Li).

Received May 15, 2023; revised June 2, 2023; accepted June 17, 2023; available online June 20, 2023.

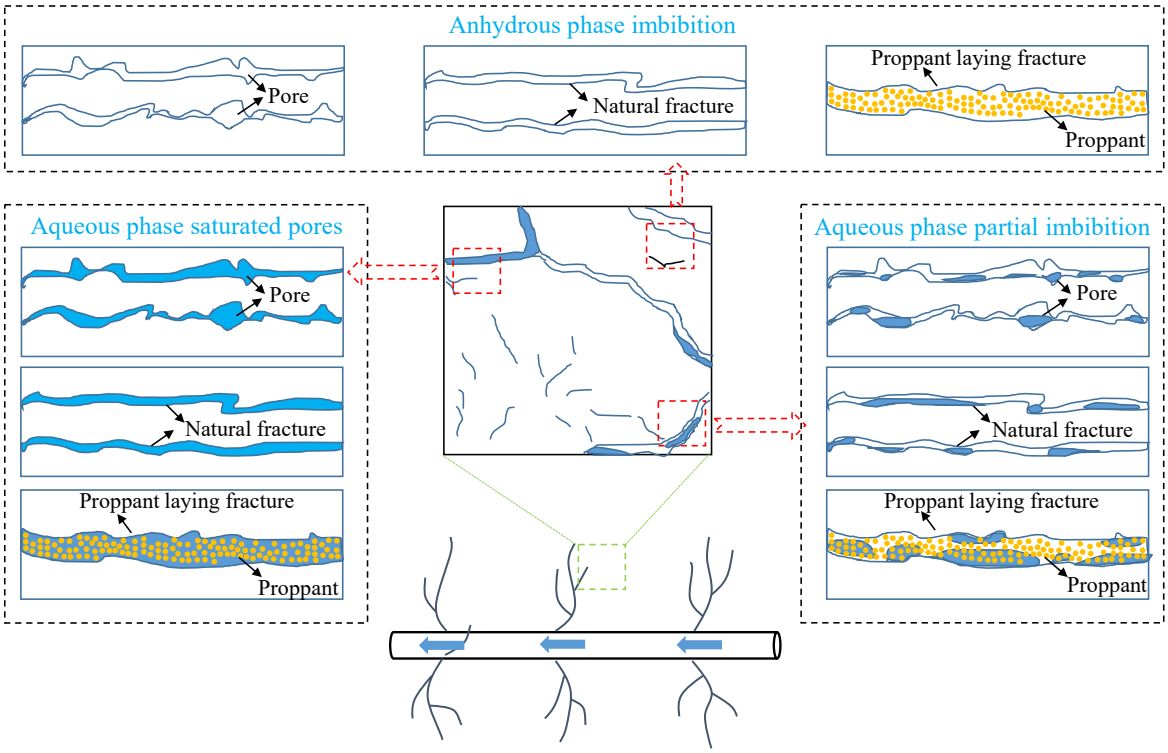

Fig. 1. Heterogeneous imbibition of fracturing fluid in a shale gas reservoir after hydraulic fracturing.

system and efficient development of shale gas wells.

At present, researches on the stress sensitivity of shale mainly focus on the flow channels of artificial fractures with proppant and natural fractures, thus can consider the hydration effect of fracturing fluid after contact with rocks, fluid sensitivity and other factors (Kang et al., 2019; Zheng et al., 2019; Liu et al., 2022). However, few studies have been conducted on the influence of fracturing fluid retention on stress sensitivity. Wang et al. (2019) explored the permeability stress sensitivity of matrix shale, while Chen et al. (2023) investigated the stress sensitivity of artificial fractures under different flowback and production processes after shutting in the well. However, neither of them considered the influence of aqueous phase imbibition. Yang et al. (2017) conducted stress sensitivity experiments on shale matrix samples considering the initial water saturation. Kang et al. (2019) studied the influence of fluid sensitivity and fracturing fluid immersion on the stress sensitivity of shale natural fractures and artificial fractures containing proppant. You et al. (2014) conducted stress sensitivity experiments on shale fractures under fracturing fluid infiltration. Meanwhile, in the above studies, the retention degree and distribution characteristics of fracturing fluid in shale multiscale pores and fractures were not considered.

The flowback of fracturing fluid is affected by spontaneous imbibition and the strong capillary force in a shale reservoir (Cai et al., 2021). Different degrees of fracturing fluid flowback lead to differences in the degree and location of fracturing fluid retention (Fig. 1), which has an important impact on multiscale mass transfer during shale gas production. Production relies on the own pressure of the shale gas reservoir. Accordingly, rock samples from a shale gas well of Longmaxi Formation were taken as the research object in this paper. Self-imbibition experiments of fracturing fluid were carried out to explore the relationship between imbibition time and imbibition capacity. Through an imbibition experiment, the distribution characteristics of different aqueous phase imbibition in shale multiscale pores and cracks were clarified. Then, according to the results of fracturing fluid imbibition experiment, a stress sensitivity experiment of shale multiscale pore structure under different imbibition and retention conditions of fracturing fluid was carried out. Through the above experiments, the stress sensitivity mechanism of a shale gas reservoir under different fracturing fluid imbibition and retention conditions was revealed.

2. Materials and methods

2.1 Shale sample properties

In order to investigate the distribution characteristics of fracturing fluid with different imbibition degrees in shale multiscale pores and fractures, cores with natural fractures taken from different depths of a shale gas well in the Longmaxi Formation, southern Sichuan Basin, were selected for the fracturing fluid imbibition experiments. In the production process, shale gas experiences a multiscale mass transfer path in the matrix, natural crack and artificial fracture with proppant. Therefore, the shale matrix core, natural fracture core and core of artificial fracture with proppant were selected from the same formation for the experiment of stress sensitivity. The cores were used to carry out the stress sensitivity experiment during the effective stress loading process. The basic parameters of the experimental samples are shown in Table 1.

Table 1. Basic parameters of shale samples.

Sample	Core type	Length (mm)	Diameter (mm)	Porosity (%)	Permeability (mD)	Test method
WR-1	Natural fracture	38.46	25.24	6.84	0.30	Imbibition
WR-2	Natural fracture	38.5	25.18	6.04	0.20	Imbibition
WR-5	Natural fracture	38.88	25.14	5.05	0.23	Imbibition
J-1	Matrix	33.2	25.4	2.97	0.0046	Stress sensitivity
J-2	Matrix	31.18	25.34	2.53	0.0026	Stress sensitivity
L-1	Natural fracture	35.6	25.3	4.3	0.21	Stress sensitivity
L-2	Natural fracture	30.9	25.5	5.6	0.24	Stress sensitivity
P-1	Proppant laying fracture	30.8	25.3	-	88.09	Stress sensitivity
P-2	Proppant laying fracture	35.5	25.4	-	79.85	Stress sensitivity

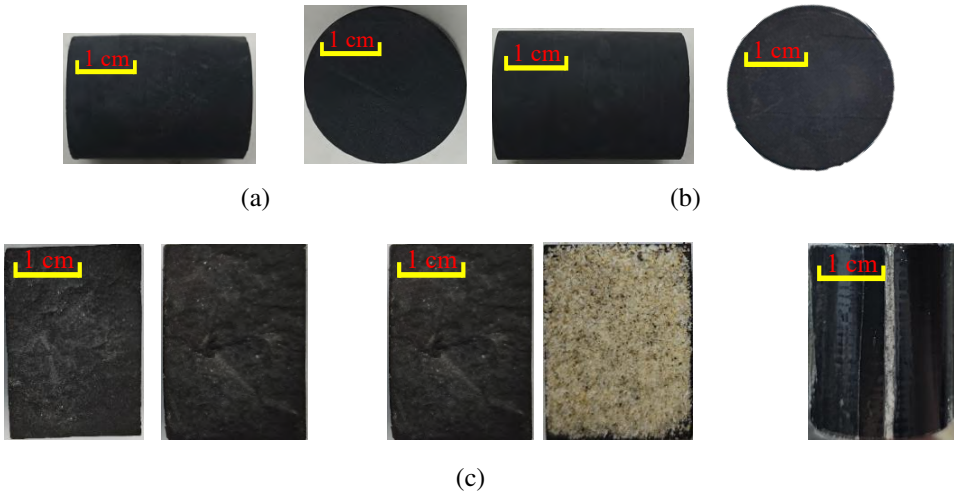

Fig. 2. Experimental core samples: (a) shale matrix core, (b) shale natueal fracture core and (c) proppant laying fracture, core fracture surface and proppant paving conditions.

The shale matrix core in this paper was a tight shale sample with permeability below 0.1 mD and no visible cracks. Natural fracture core refers to the core surface that developed natural fractures, visible to the naked eye and is not penetrated. The cores of artificial fracture with proppant were prepared according to the type of proppant and the proppant laying concentration under in-situ conditions. A certain proportion of 40-200 mesh quartz sand was selected and evenly laid on the artificial fracture surface, and the proppant paving density was 0.5 kg/m^2. After the proppant laying was completed, the core was wrapped with a heat shrink film. The three types of cores are shown in Fig. 2.

2.2 Experimental principle and test method

Parts of the fracturing fluid in a shale gas well can be subject to flowback after hydraulic fracturing, and there are differences in the degree of retention of aqueous phase in the complex micron-nano flow channels of the reservoir. To characterize the stress sensitivity characteristics of the shale gas reservoir under the conditions of fracturing fluid imbibition and retention, it is necessary to reveal the distribution characteristics of fracturing fluid in multiscale pores and fractures under different water conditions.

The amount of shale sample imbibition varies between different time points, and the distribution position of fracturing fluid in shale pore structure is also different. In this paper, the shale samples were fully immersed in distilled water to simulate fracturing fluid imbibition. Full immersion imbibition effectively avoids the influence of imbibition due to the drilling direction of rock samples (Zhou et al., 2022). Then, according to the results of the imbibition experiment, the stress sensitivity experiment of shale under different imbibition time was designed.

The experiments were divided into two groups. The fracturing fluid imbibition experiments of shale consisted the first group, and the stress sensitivity experiments of shale under different water imbibition conditions comprised the second group.

The imbibition experimental process was conducted as follows:

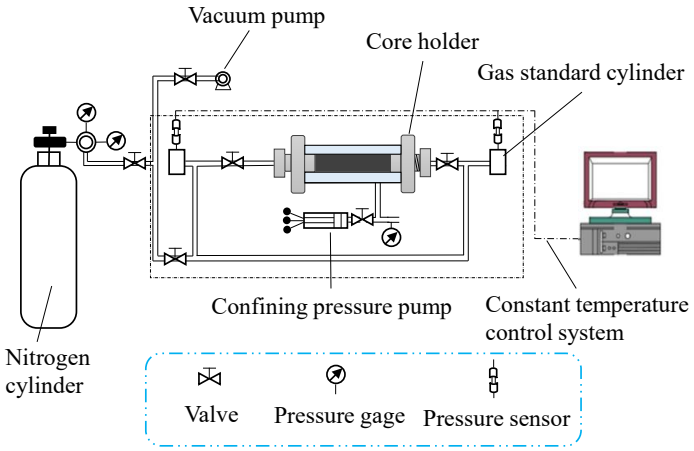

Fig. 3. Flowchart of the pressure pulse attenuation permeability tester.

(1) The shale core was dried at 110 °C for 24 h and then weighed. A nuclear magnetic resonance (NMR) analysis system was implemented to measure the T_2 pattern of dry cores.

(2) The shale cores WR-2, WR-1 and WR-5 were fully immersed in fracturing fluid for imbibition, and the imbibition time was set to 10, 20 and 30 min, separately. Most of the shale fracturing fluids use a slickwater system (Denney et al., 2010; Jacobs et al., 2019; Ai-Hajri et al., 2022), and more than 90% of the system is aqueous phase, so distilled water was used to simulate the slickwater fracturing fluid. The amount of shale imbibition at each time point was measured by taking out samples at certain time intervals and weighing them. After the completion of imbibition, the NMR analysis system was employed to test the distribution of aqueous phase in the multiscale pore and the fracture structure of shale.

(3) The shale samples were dried by repeating Step (1), the three experimental samples were fully immersed for 120, 720 and 1,440 min, and the aqueous phase distribution characteristics were analyzed by NMR instrument.

(4) The core was dried and vacuumed in a ZB-2 core vacuum saturation device for 4 h. Next, the core was saturated with pressure imbibition of distilled water for 12 h, and the saturation pressure was 20 MPa. The core pore size distribution was measured by the NMR analysis system.

The multiscale pore and fracture stress sensitivity experiments of shale under different aqueous phase distribution conditions were carried out as follows:

(1) The shale samples were dried at 110 °C for 24 h, and the dry weight of cores were weighed.

(2) Based on the above fracturing fluid imbibition experiment, the aqueous phase imbibition experiments of the core of matrix, core of natural fracture and core of artificial fracture with proppant were carried out at different set times, and the fracturing fluid retention in the pore space of a shale reservoir at different scales was simulated during the flowback process after hydraulic fracturing of a shale gas well.

(3) The permeability under different effective stresses was tested by pressure pulse decay method for matrix cores and natural fracture cores. The experimental instruments are shown in Fig. 3. The experimental steps were as follows:

a) Place the core in a core holder and apply confining pressure to the core.

b) Vacuum the experimental system for 24 h. Then, inject a certain amount of nitrogen into the two sections of the core gripper, and close the intake valve and gas source.

c) Detect the gas pressure decay process, and stop the pressure data acquisition once the test pressure is basically stable.

d) Open the vent valve, discharge the excess nitrogen, change the core confining pressure, and repeat the above experimental steps. Set the effective stress separately to 3, 5, 10, 15 and 20 MPa. To eliminate the effect of time on stress sensitivity, stress is maintained for more than 4 h after reaching each stress point.

(4) The gas-measured permeability under different effective stresses was obtained by the steady-state method for the artificial fracture pore with proppant. The effective stress was separately set to 3, 5, 10, 15, 20 and 30 MPa. Each stress point was kept for $>$ 30 min to eliminate the stress sensitivity time effect.

(5) The degree of permeability damage was calculated and the multiscale pore and fracture stress sensitivity of a shale gas reservoir after hydraulic fracturing was evaluated.

3. Imbibition characteristics

3.1 Imbibition capacity at different time points

Fig. 4 shows the relationship between the uptake amount of fracturing fluid in unit mass of shale and the time of imbibition. The imbibition curve shows a rapid rising trend followed by a slow increase. In the first 2 h of the core imbibition experiment, the imbibition capacity increases rapidly. Especially in the first 20 minutes of infiltration, the amount

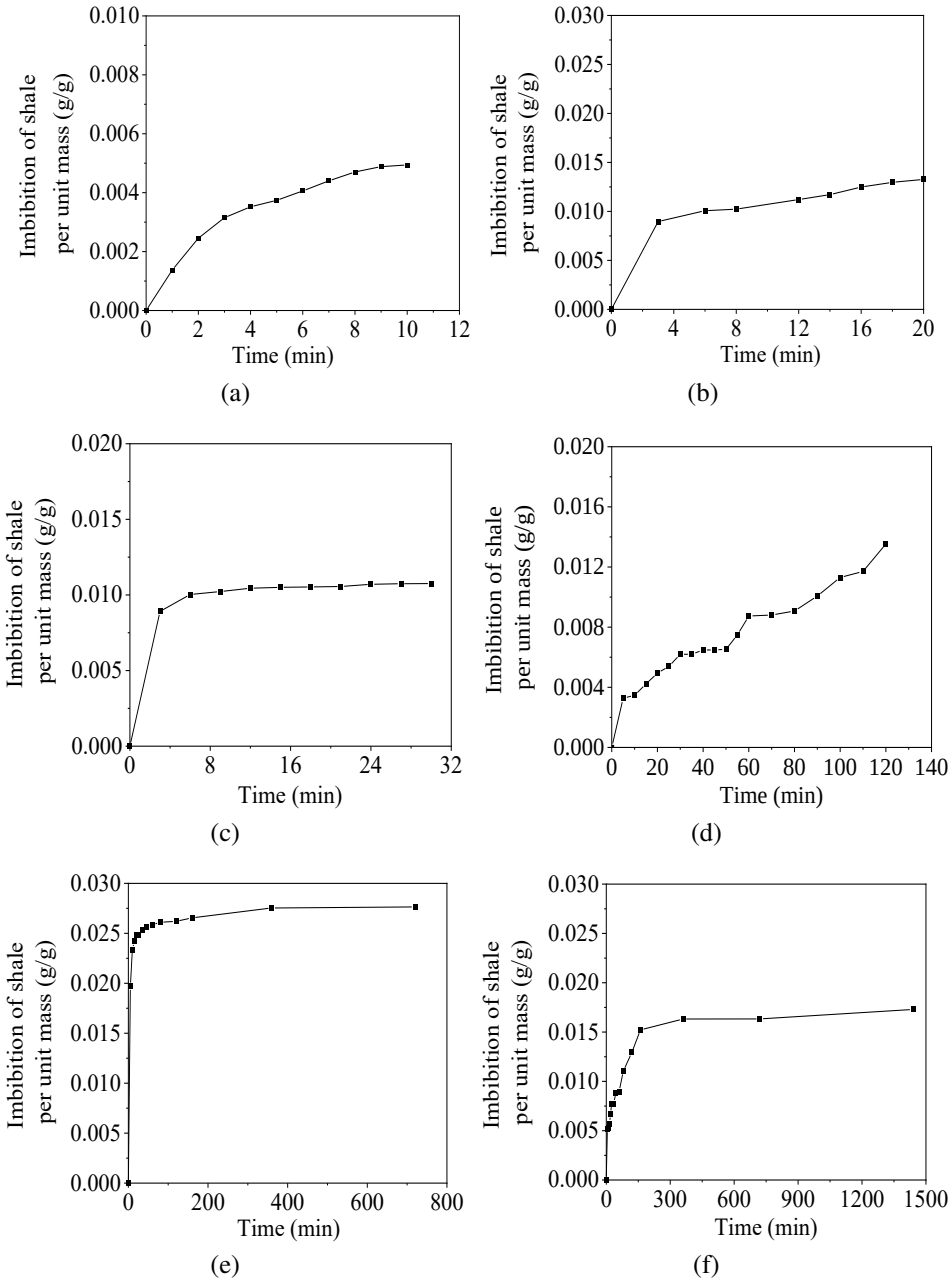

Fig. 4. Relationship between imbibition time and per unit mass of shale: (a) imbibition for 10 min of sample WR-2, (b) imbibition for 20 min of sample WR-1, (c) imibibition for 30 min of sample WR-5, (d) imbibition for 120 min of sample WR-2, (e) imbibition for 720 min of sample WR-1 and (f) imbibition for 1,440 min of sample WR-5.

of WR-1, WR-2 and WR-5 unit mass imbibition is 0.01327, 0.00494 and 0.00669, respectively, reaching about 50% of the cumulative unit mass imbibition of the cores. However, after 2 h, the imbibition rate slows down, and the amount of imbibition per unit mass increases slowly.

3.2 Fracturing fluid distribution

The distribution of aqueous phase in shale multiscale pore and fracture structure at different imbibition times was tested by full-diameter core NMR analysis system. Fig. 5 illustrates a distribution diagram of the imbibition aqueous phase in the multiscale pore space of shale according to the NMR T_2 process. This result indicates that when the water saturation is low, the aqueous phase preferentially fills the shale nanoscale pores under the action of capillary force. On the other hand, when the water saturation increases gradually, the aqueous phase enters the micron-scale pore space. In this paper, the pore volume multiple was used to characterize the amount of imbibition phase in a shale. According to the intensity of NMR peaks, the pore volume multiples of imbibition at 10, 20, 30, 120, 720 and 1,440 min were 0.52, 0.55, 0.64, 0.78, 0.9, and 0.96 pore volume (PV), respectively (Fig. 5).

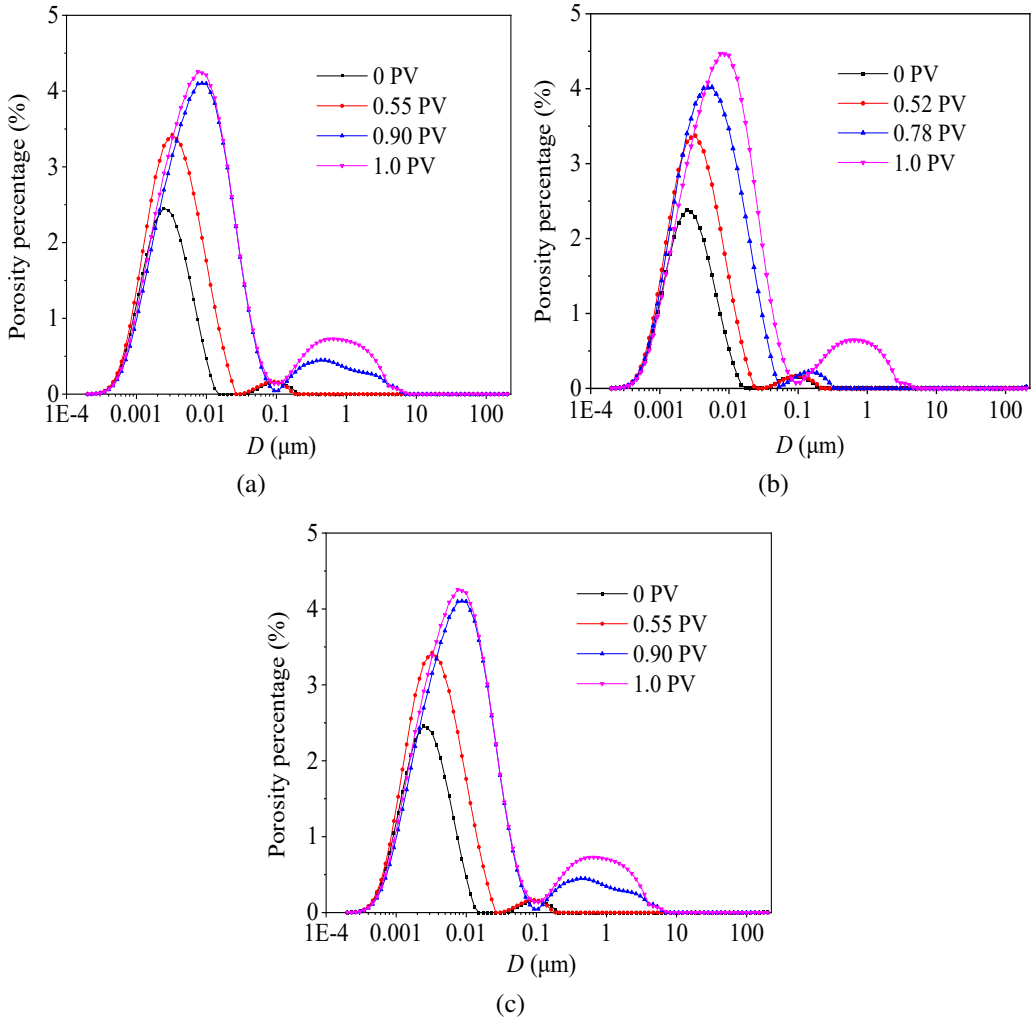

Fig. 5. NMR T_2 diagrams of shale samples with different degrees of aqueous phase: (a) WR-1, (b) WR-2 and (c) WR-5.

The shale pore size (diameter) can be divided into the following five categories: < 2 nm (micropore), 2-50 nm (mesopore), 50-100 nm (macropore), 100-1,000 nm (submicron pore), > 1,000 nm (micron pore) (Chen et al., 2017; Zhong et al., 2019). The statistical analyses of the distribution characteristics of aqueous phase in the shale multiscale pores and fractures are shown in Fig. 6. The results indicate that when the water saturation reaches 0-0.78 PV, the aqueous phase mainly enters the 2-50 nm mesopores, and partly enters the < 2 nm micropores. Water saturation at the pore/fracture sizes of 50-100, 100-1,000 and > 1,000 nm is higher than that in dry samples, while the increase is relatively small. When the water saturation in pores increases to more than 0.9 PV, the water saturation in 100-1,000 nm submicron pores and > 1,000 nm micron pores increases significantly.

4. Shale stress sensitivity under imbibition

The micron/nanoscale pore and fracture structure of shale is the material basis of multiscale mass transfer (Chen et al., 2018), and the degree and location of fracturing fluid retention has an important impact on the stress sensitivity of a shale gas reservoir.

Based on the results of the above imbibition experiment of shale, the distribution of aqueous phase in shale multiscale pore and fracture under different imbibition times was used to simulate the different aqueous phase flowback degree after hydraulic fracturing. The case of complete flowback of fracturing fluid corresponds to the aqueous phase imbibition of 0 PV. Aqueous phase imbibition with 0.9 PV was used to simulate the partial fracturing fluid flowback, and the aqueous phase was mainly distributed in mesopores between 2 and 50 nm. The fracturing fluid that is basically not returned corresponds to 0.9-1 PV, and the aqueous phase exists in multiscale pores and fractures. Therefore, core stress sensitivity tests under different degrees of fracturing fluid retention were carried out by using dry samples, 20 and 1,440 min self-imbibition core, natural fracture core, and artificial fracture core with proppant.

4.1 Stress sensitivity of the matrix

Based on the core permeability test results applied for 4 h under the effective stress condition of 3 MPa, the normalized permeability of each effective stress point during the increase

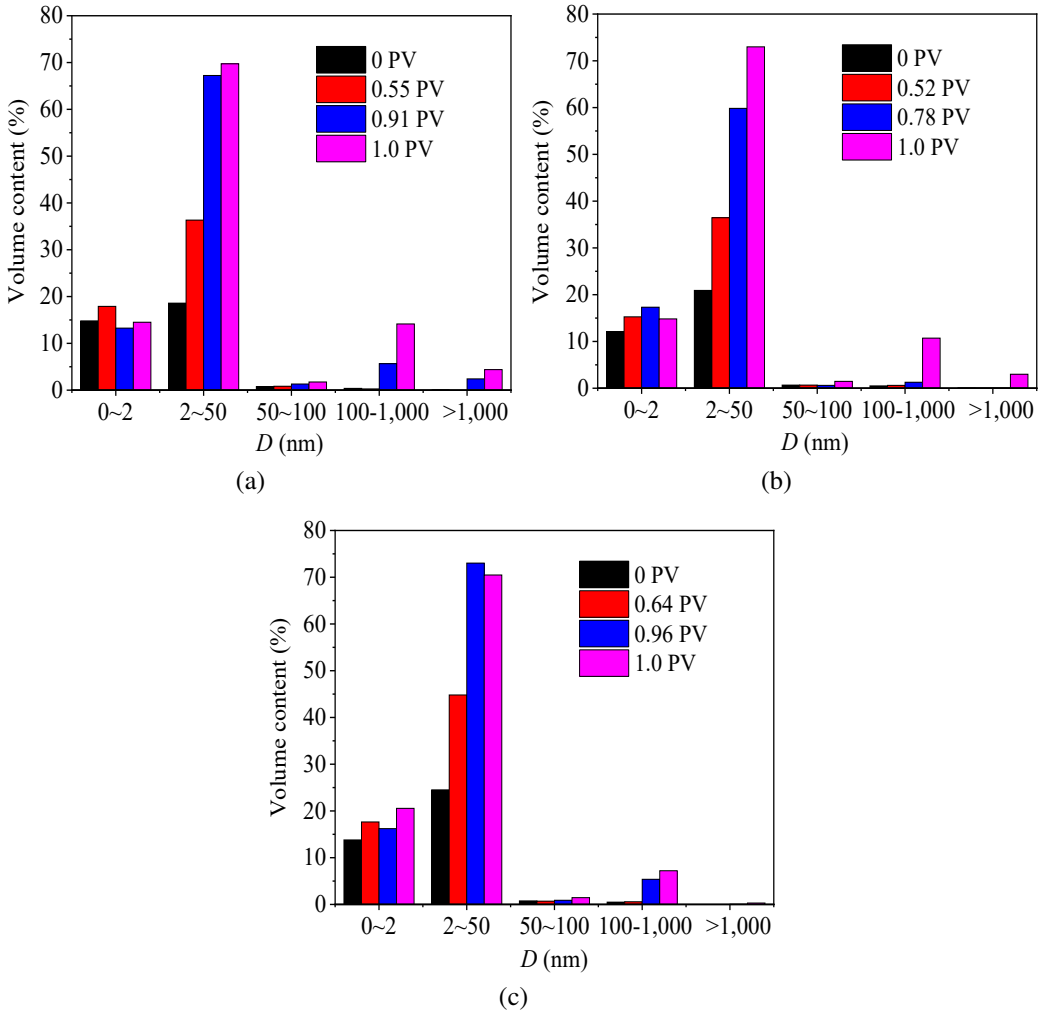

Fig. 6. Characteristics of aqueous phase distribution in the multiscale flow channels of shale: (a) WR-1, (b) WR-2 and (c) WR-5.

in effective stress was calculated.

Under the effective stress of 20 MPa, the average permeability damage rates of J-1 and J2 matrix cores under the conditions of dry sample and fracturing fluid imbibition for 20 and 1,440 min were 42.19%, 73.83% and 76.53%, respectively. In the process of effective stress increase, the permeability damage rate of the shale matrix presents the following law: dry sample < imbibition for 20 min < imbibition for 1,440 min. Meanwhile, the permeability damage degree of the matrix sample increases with an elevating degree of fracturing fluid retention.

Under the same effective stress, the permeability damage of matrix core J-1 and J-2 from dry sample to fluid imbibition for 20 min was significantly higher than that from imbibition for 20 to 1,440 min. In other words, it could be established that when the aqueous phase in the matrix core ranges from 0 to 0.5 PV, the damage to the core permeability is more severe than that when the occurrence rises from 0.5 to 0.9 PV. This trend becomes more pronounced as the effective stress increases (Fig. 7). According to the experimental results in Section 3.2, when the saturation degree of aqueous phase increases from 0 to 0.5 PV, the aqueous phase mainly exists in the pore size of 2-50 nm. Therefore, fracturing fluid retention in pores of 2-50 nm has a more significant impact on the permeability damage of shale matrix.

4.2 Stress sensitivity of natural fracture

Under the effective stress of 20 MPa, the average permeability damage rates of L-1 and L-2 natural fracture cores under the conditions of dry sample and fracturing fluid imbibition for 20 and 1,440 min were 75.86%, 84.56% and 95.97%, respectively. The change trend of permeability damage rate of natural fracture core with the increase in effective stress was basically the same as that of matrix core, which is dry sample < imbibition for 20 min < imbibition for 1,440 min. In other words, the stress sensitivity of natural fractures increases with rising fracturing fluid retention.

Fracturing fluid imbibition and retention in a shale gas reservoir have a double effect on shale permeability. On the one hand, water-rock interaction inducing micro-crack initiation and expansion can occur (Ogata et al., 2018; Zhou et al., 2021; Li et al., 2023). On the other hand, this can

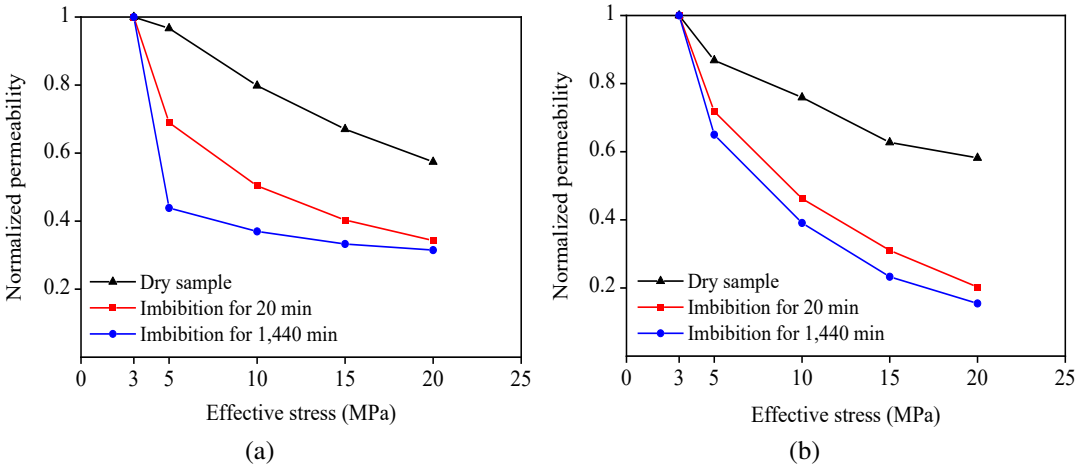

Fig. 7. Permeability retention rates of (a) J-1 and (b) J-2 shale matrix core during the increase in effective stress.

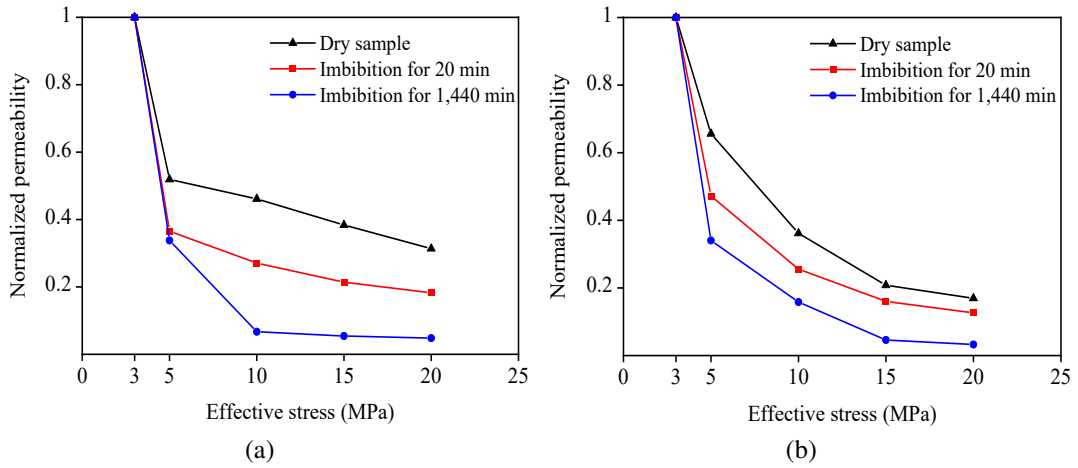

Fig. 8. Permeability retention rates of (a) L-1 and (b) L-2 in shale natural fracture cores during effective stress increase.

cause aqueous phase trapping damage and block the gas flow channel, resulting in decreased permeability (Abaa et al, 2017; Zhong et al., 2019; Chen et al., 2021). With the effective stress increasing from 3 to 5 MPa, the permeability of matrix core J-1 and natural fracture core L-1 and L-2 under the condition of water imbibition dropped sharply. After 20 min of imbibition, the aqueous phase saturation increased from 0 to about 0.5 PV, and the average normalized permeability decreased by 49.11%. Under the imbibition condition of 1,440 min, the aqueous phase saturation reached about 0.9 PV, and the average normalized permeability decreased by 62.77% (Figs. 7 and 8). This occurred precisely because the microcracks induced by aqueous phase imbibition were compacted, and the permeability decreased more significantly with the increase in the aqueous phase retention degree.

For natural fracture cores, the increase degree of permeability damage of L-1 and L-2 under the same effective stress from 20 to 1,440 min was higher than that under the condition from dry sample to 20 min. That is to say, the degree of natural fracture core damage increase is more serious when the aqueous phase occurrence rises from 0.5-0.9 PV than when it rises from 0-0.5 PV. This shows that aqueous phase retention in 100-1,000 and > 1,000 nm pores plays a leading role in the permeability damage of shale natural fracture cores.

The normalized permeability of each effective stress point in the process of effective stress increase was calculated by taking the core permeability test result of 4 h applied to the natural fracture core under the condition of 3 MPa effective stress as the initial permeability.

4.3 Stress sensitivity of artificial fracture with proppant

The average permeability damage rates of P-1 and P-2 artificial fracture cores with proppant under 30 MPa effective stress were 66.37%, 53.93% and 48.09%, respectively, under the conditions of dry sample and fracturing fluid imbibition for 20 min and 1,440 min. The core permeability damage rate showed the law of dry sample > imbibition for 20 min > imbibition for 1,440 min.

Under the same effective stress condition, the permeability damage rate of the artificial fracture cores with proppant did not completely present the above law. However, with the load-

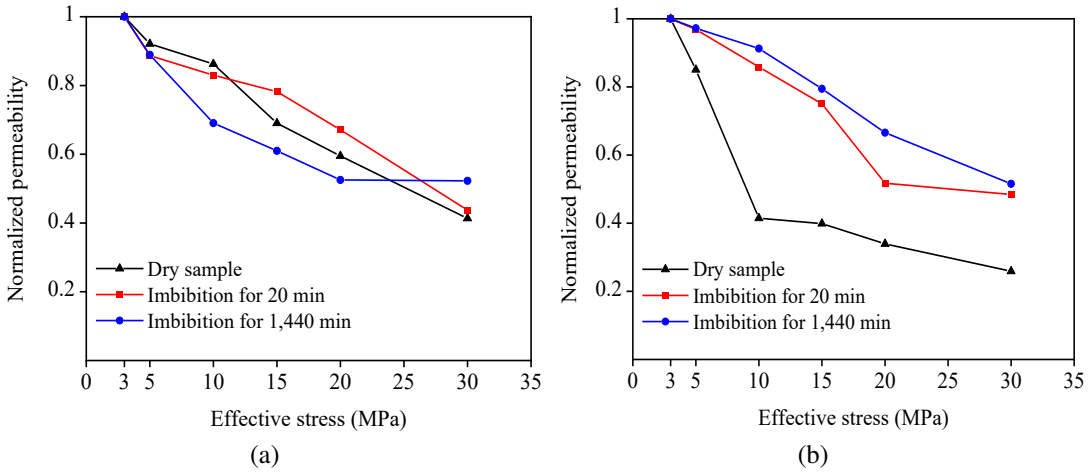

Fig. 9. Permeability retention rates of (a) P-1 and (b) P-2 of artificial fracture cores with proppant during the process of effective stress increase.

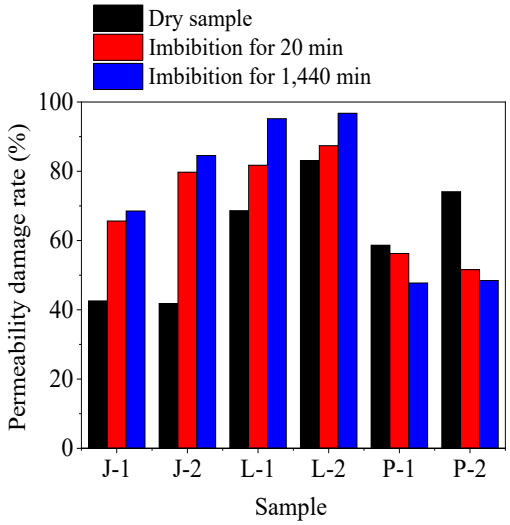

Fig. 10. Shale permeability damage rate under an effective stress of 20 MPa.

ing of effective stress, the permeability of dry sample decreased more than that under the conditions of imbibition and retention of fracturing fluid. Proppant intrusion into the fracture surface and proppant breakage were the main mechanisms of stress sensitivity of artificial fracture cores with proppant. Combined with the results of stress sensitivity experiment for the cores of artificial fracture with proppant (Fig. 9), it is indicated that under the condition of lower effective stress (< 10 MPa), the proppant on the fracture surface with a certain moisture content might be more invasive than that on the dry crack surface. Under higher effective stress conditions (> 10 MPa), the less water content in the crack surface, the more likely the proppant could break or invade into the fracture surface, making the stress sensitivity stronger.

Taking the core permeability test result after 30 min under the effective stress condition of 3 MPa as the initial permeability, the normalized permeability of each effective stress point during the increase of effective stress was calculated.

Table 2. Increase in the average permeability damage rate of matrix cores after imbibition for 20 min (compared with damage rate of dry sample).

Core type	Permeability damage rate (%)			
	5 MPa	10 MPa	15 MPa	20 MPa
Matrix	21.38	29.58	29.23	31.65
Natural fracture	16.90	14.83	10.88	8.71

Table 3. Increase in the average permeability damage rate of matrix cores after imbibition for 1440 min (compared with damage rate of 20 min imbibition).

Core type	Permeability damage rate (%)			
	5 MPa	10 MPa	15 MPa	20 MPa
Matrix	15.96	10.29	7.39	2.7
Natural fracture	7.94	15.05	13.69	11.41

5. Discussion

Stress sensitivity is aggravated by fracturing fluid retention in the matrix nanopores and natural fractures, while the effect of different fracturing fluid retention degrees on stress sensitivity in the multiscale pore structure is also different. From the perspective of permeability damage degree, as shown in Fig. 10, the normalized permeability damage rate of natural fracture cores under the condition of aqueous phase retention is greater than that of matrix cores. As for the degree of permeability damage aggravated by different retention values of fracturing fluid, under different effective stress conditions, the average permeability damage rate of the matrix core increases by 27.96% and that of natural fracture core increases by 12.83% when the aqueous phase retention is 0.5 PV (Tables 2 and 3). In other words, when the aqueous phase is about 0.5

PV, the stress sensitivity of the matrix core is higher than that of the natural fracture core. However, with the increase in aqueous phase retention, the stress sensitivity of natural fractures becomes more serious. During the shut-in period of a shale gas well, the aqueous phase can gradually migrate into increasingly smaller pore spaces (Zhou et al., 2018b; Wijaya and Sheng, 2020; Cai et al., 2022). This self-migration of the aqueous phase is due to the effect of capillary force (Liu et al., 2016; Liang et al., 2021; Wang et al., 2022). The aqueous phase remains in 100-1,000 and $>$ 1,000 nm pores or fractures, and migrates into of 2-50 and $<$ 2 nm pores. Such behavior can cause the water trapped in the natural fracture to transfer to the matrix after flowback, weakening the stress sensitivity of the fracturing fluid to natural fracture.

The shale gas production mode relies on the pressure of the shale gas reservoir, which causes the effective stress of the reservoir to increase gradually. The increased sensitivity of fracturing fluid retention to matrix and natural fracture stress may be one of the main reasons for the high production of a shale gas well in the early stage of production, followed by a rapid decline. In the actual development process, the stress sensitivity in a shale gas reservoir with multiscale pores and fractures should be paid more attention. Based on the stress sensitivity test results of flow channels of different scales, a reasonable shut-in time and drainage system should be established. In this way, fracturing fluid intrusion can be controlled within a reasonable range and fracturing fluid flowback in matrix-natural fractures can be promoted. However, in the production process of a shale gas well, it is not practical to completely allow the flowback of fracturing fluid in the matrix pores and natural fractures. Instead, it is recommended to control the retained fracturing fluid in a shale gas reservoir as far below 0.5 PV as possible. On the one hand, the stress sensitivity of fracturing fluid retention to natural fractures is relatively low, and the stress sensitivity of artificial fractures with proppant is alleviated to a certain extent. On the other hand, 2-50 and $<$ 2 nm pores in the matrix have the space to accommodate the self-migrating aqueous phase in the natural cracks. Thus, it is beneficial to alleviate reservoir stress sensitivity and aqueous phase trapping damage caused by fracturing fluid retention, and promote the high and stable production of the shale gas well.

6. Conclusions

1) When the water saturation is 0-0.78 PV, the aqueous phase mainly enters the mesopores of 2-50 nm. When the water saturation of the core reaches more than 0.9 PV, the water saturation of the 100-1,000 nm submicron pores and the 1,000 nm micropores increases significantly.
2) Under the same effective stress, the permeability damage rate of matrix and natural fracture core is proportional to the degree of imbibition and retention of fracturing fluid. Meanwhile, under different effective stress conditions, when the aqueous phase retention is 0.5 PV, the average permeability damage rate of matrix core increases by 27.96%, and that of natural fracture core increases by 12.83%. When the aqueous phase retention degree rises to about 0.9 PV, the average permeability damage rate of matrix core increases by 9.09%, and that of natural fracture core increases by 12.02%.
3) The imbibition and retention of fracturing fluid in the 2-50 nm pores contribute significantly to the permeability damage of shale matrix samples. Aqueous phase retention in flow channels larger than 100 nm in shale natural fracture cores is the leading factor to increase the permeability damage.
4) It is recommended to control the fracturing fluid retention below 0.5 PV in a shale gas reservoir. It is helpful to alleviate the reservoir stress sensitivity aggravated by fracturing fluid retention and aqueous phase trapping damage to a certain extent, which can promote the stable production of a shale gas well.

Acknowledgements

The current research was supported by the National Natural Science Foundation of Sichuan, China (No. 2023NSFSC0939) and the Open Fund (No. PLN2022-11) of the State Key Laboratory of Oil and Gas Reservoir Geology and Exploitation (Southwest Petroleum University). The editors and reviewers of the journal have put forward many constructive comments on this paper, for which we would like to express our sincere thanks.

Conflict of interest

The authors declare no competing interest.

References

Abaa, K., Thaddeus, M., Adewumi, M. Effect of acoustic stimulation on aqueous phase trapping in low-permeability sandstones. Journal of Energy Resources Technology, 2017, 139(6): 062905.

Ai-Hajri, S., Negash, B., Rahman, M., et al. Perspective Review of polymers as additives in water-based fracturing fluids. ACS Omega, 2022, 7(9): 7431-7443.

Cai, J., Chen, Y., Liu, Y., et al. Capillary imbibition and flow of wetting liquid in irregular capillaries: A 100-year review. Advances in Colloid and Interface Science, 2022, 304: 102654.

Cai, J., Jin, T., Kou, J., et al. Lucas-Washburn equation-based modeling of capillary-driven flow in porous systems. Langmuir, 2021, 37(5): 1623-1636.

Chen, L., Jiang, Z., Liu, K., et al. Quantitative characterization of micropore structure for organic-rich Lower Silurian shale in the Upper Yangtze Platform, South China: Implications for shale gas adsorption capacity. Advances in Geo-Energy Research, 2017, 1(2): 112-123.

Chen, M., Kang, Y., Zhang, T., et al. Characteristics of multiscale mass transport and coordination mechanisms for shale gas. Scientia Sinica Technologica, 2018, 48(5): 473-487. (in Chinese)

Chen, M., Li, P., Kang, Y., et al. Effect of aqueous phase trapping in shale matrix on methane sorption and diffusion capacity. Fuel, 2021, 289: 119967.

Chen, H., Wei, J., Cheng, H., et al. Stress densitivity of proppant-containing fractures and its influence on fas well productivity. Geofluids, 2023, 2023: 8851149.

Denney, D. Tight reservoirs: Proppant transport in slickwater fracturing of shale-gas formations. Journal of Petroleum Technology, 2010, 62(10): 56-69.

Edwards, R., Celia, M. Shale gas well, hydraulic fracturing, and formation data to support modeling of fas and water flow in shale formations. Water Resources Research, 2018, 54(4): 3196-3206.

Gasparik, M., Ghanizadeh, A., Bertier, P., et al. High-pressure methane sorption isotherms of black shales from the Netherlands. Energy & Fuels, 2012, 26(8): 4995-5004.

Han, D., Wang, H., Wang, C., et al. Differential characterization of stress sensitivity and its main control mechanism in deep pore-fracture clastic reservoirs. Scientific Reports, 2021, 11(1): 7374.

Jacobs, T. Shale sector's switch to slickwater highlights compatibility issues with produced water. Journal of Petroleum Technology, 2019, 71(11): 31-32.

Kang, Y., Bai, J., Li, X., et al. Influence of water-rock interaction on stress sensitivity of organic-rich shales: A case study from Longmaxi formation in the southeast area of Chongqing. Petroleum Reservoir Evaluation and Development, 2019, 9(5): 54-62. (in Chinese)

Li, N., Jin, Z., Wang, H., et al. Investigation into shale softening induced by water/CO_2-rock interaction. International Journal of Rock Mechanics and Mining Sciences, 2023, 161: 105299.

Liang, Y., Lai, F., Dai, Y., et al. An experimental study of imbibition process and fluid distribution in tight oil reservoir under different pressures and temperatures. Capillarity, 2021, 4(4): 66-75.

Lin, H., Yang, B., Song, X., et al. Fracturing fluid retention in shale gas reservoir from the perspective of pore size based on nuclear magnetic resonance. Journal of Hydrology, 2021, 601: 126590.

Liu, D., Ge, H., Liu, J., et al. Experimental investigation on aqueous phase migration in unconventional gas reservoir rock samples by nuclear magnetic resonance. Journal of Natural Gas Science and Engineering, 2016, 36(A): 837-851.

Liu, J., Liu, J., Liu, H., et al. Mechanism study on release of "Water blocking damage" of tight sandstone by nano fluid and case study. Paper ARMA 2020-1041 Presented at the 54th U.S. Rock Mechanics/Geomechanics Symposium, physical event cancelled, 28 June-1 July, 2020.

Liu, X., Pan, Y., Li, M., et al. Permeability of hydrated shale rocks under cyclic loading and unloading conditions. Journal of China Coal Society, 2022, 47(S1): 103-114. (in Chinese)

Ogata, S., Yasuhara, H., Kinoshita, N., et al. Modeling of coupled thermal-hydraulic-mechanical-chemical processes for predicting the evolution in permeability and reactive transport behavior within single rock fractures. International Journal of Rock Mechanics and Mining Sciences, 2018, 107: 271-281.

Rashid, S., Boyun, G., Philip B., et al. Stress-sensitivity of fracture conductivity of Tuscaloosa Marine Shale cores. Journal of Petroleum Science and Engineering, 2022, 210: 110042.

Shaoul, L., Zelm, V., Pater, C. Damage mechanisms in unconventional-gas-well stimulation a new look at an old problem. SPE Production & Operation, 2011, 26(4): 388-400.

Sheng, G., Wang, W., Zhao, H., et al. Study of fracturing fluid imbibition impact on gas-water two phase flow in shale fracture-matrix system. Paper URTEC 2020-3323 Presented at the SPE/AAPG/SEG Unconventional Resources Technology Conference, Virtual, 20-22 July, 2020.

Shi, W., Zhang, C., Jiang, S., et al. Study on pressure-boosting stimulation technology in shale gas horizontal wells in the Fuling shale gas field. Energy, 2022, 254: 124364.

Wang, Y., Kang, Y., Wang, D., et al. Liquid phase blockage in micro-nano capillary pores of tight condensate reservoirs. Capillarity, 2022, 5(1): 12-22.

Wang, X., Zhu, Y., Fu, C., et al. Experimental investigation of the stress-dependent permeability in the Longmaxi Formation shale. Journal of Petroleum Science and Engineering, 2019, 175: 932-947.

Wijaya, N., Sheng, J. Shut-in effect in removing water blockage in shale-oil reservoirs with stress-dependent permeability considered. SPE Reservoir Evaluation & Engineering, 2020, 23(1): 81-94.

Xu, Y., Liu, X., Hu, Z., et al. Bottom-hole pressure drawdown management of fractured horizontal wells in shale gas reservoirs using a semi-analytical model. Scientific Reports, 2022, 12(1): 22490.

Yang, L., Wang, S., Cai, J., et al. Main controlling factors of fracturing fluid imbibition in shale fracture network. Capillarity, 2018, 1(1): 1-10.

Yang, D., Wang, W., Chen, W., et al. Experimental investigation on the coupled effect of effective stress and gas slippage on the permeability of shale. Scientific Reports, 2017, 7(1): 44696.

You, L., Wang, Q., Kang, Y., et al. Influence of fracturing fluid immersion on stress sensitivity of shale reservoir. Petroleum Geology and Recovery Efficiency, 2014, 21(6): 102-106. (in Chinese)

Zeng, F., Zhang, Q., Guo, J., et al. Capillary imbibition of confined water in nanopores. Capillarity, 2020, 3(1): 8-15.

Zhang, Y., Ge, H., Shen, Y., et al. The retention and flowback of fracturing fluid of branch fractures in tight reservoirs. Journal of Petroleum Science and Engineering, 2021, 198: 108228.

Zhang, W., Wang, Q., Ning, Z., et al. Relationship between the stress sensitivity and pore structure of shale. Journal of Natural Gas Science and Engineering, 2018, 59: 440-451.

Zheng, X., Zhang, B., Sanei, H., et al. Pore structure characteristics and its effect on shale gas adsorption and desorption

behavior. Marine and Petroleum Geology, 2019, 100: 165-178.

Zhong, Y., Zhang, H., Kuru, E., et al. Mechanisms of how surfactants mitigate formation damage due to aqueous phase trapping in tight gas sandstone formations. Colloids and Surfaces A: Physicochemical and Engineering Aspects, 2019, 573: 179-187.

Zhou, X., Chen, D., Xia, Y., et al. Spontaneous imbibition characteristics and influencing factors of Chang 7 shale oil reservoirs in Longdong Area, Ordos Basin. Earth Science, 2022, 47(8): 3045-3055. (in Chinese)

Zhou, M., Li, J., Luo, Z., et al. Impact of water-rock interaction on the pore structures of red-bed soft rock. Scientific Reports, 2021, 11(1): 7398.

Zhou, S., Ning, Y., Wang, H., et al. Investigation of methane adsorption mechanism on Longmaxi shale by combining the micropore filling and monolayer coverage theories. Advances in Geo-Energy Research, 2018a, 2(3): 269-281.

Zhou, Z., Teklu, T., Li, X., et al. Experimental study of the osmotic effect on shale matrix imbibition process in gas reservoirs. Journal of Natural Gas Science and Engineering, 2018b, 49: 1-7.

Zou, C., Pan, S., Jing, Z., et al. Shale oil and gas revolution and its impact. Acta Petrolei Sinica, 2020, 41(1): 1-12. (in Chinese)